Food Chemistry Advances 1 (2022) 100123

Contents lists available at ScienceDirect

Food Chemistry Advances

journal homepage: www.elsevier.com/locate/focha

Effects of pH, protein:polysaccharide ratio, and NaCl-added concentration on whey protein isolate and soluble soybean polysaccharides electrostatic-complexes formation

Daniela E. Igartúa[a,b], Dario M. Cabezas[a,b], Gonzalo G. Palazolo[a,b,*]

[a] Departamento de Ciencia y Tecnología, Laboratorio de Investigación en Funcionalidad y Tecnología de Alimentos (LIFTA), Universidad Nacional de Quilmes, Roque Sáenz Peña 352, B1876BXD, Bernal, Buenos Aires, Argentina

[b] Consejo Nacional de Investigaciones Científicas y Técnicas (CONICET), Godoy Cruz 2290, Ciudad Autónoma de Buenos Aires C1425FQB, Argentina

ARTICLE INFO

Keywords:
Whey protein
Soy polysaccharides
Biopolymer interactions
Electrostatic assembly

ABSTRACT

In the present work, the interaction between whey protein isolate (WPI) and soluble soybean polysaccharide (SSPS) was studied as a function of pH (7.0 to 2.0), WPI:SSPS mass ratio (1:1 to 10:1), and NaCl-added concentration (0 to 100 mM). The interaction was analyzed by ζ-potential, turbidity, and state diagrams. Then, WPI-SSPS complexes were obtained in the optimized conditions of pH (4.0 to 3.5), WPI:SSPS ratio (2:1 to 6:1), and NaCl-added concentration (0 to 100 mM). The complexes were characterized by ζ-potential, particle size, and physical stability in a factorial 3×3 design with analysis by response surface methodology. This methodology showed that the characteristics of the WPI-SSPS complexes are modulated by the modification of the studied parameters. By lowering the pH, the complexes showed a ζ-potential closer to 0 and higher physical stability. By decreasing the WPI:SSPS ratio, the complexes showed more negative ζ-potential. Finally, by increasing the NaCl concentration, the complexes showed negative ζ-potential but an increment of mean particle size and polydispersity index. Data obtained in this work is useful to design WPI-SSPS complexes with specific characteristics of size, charge, and physical stability. These complexes could then be applied in food, medicinal or cosmetic matrices for different purposes.

1. Introduction

Whey is an important low-cost by-product of the cheese and yogurt industries, which produce it in bulk amounts. Both industries and academic research have been researching ways to valorize it since potential health benefits ranging from antibacterial effects to human cognitive development and gut health has been reported (Rocha-Mendoza et al., 2021). A valuable by-product of whey revalorization is whey protein isolate (WPI), which is frequently used in foods due to its nutritional value and techno-functional properties, including emulsification, water holding, and gelling. WPI is mainly composed of β-lactoglobulin (~80%; MW: 18.3 kDa) and α-lactalbumin (~12%; MW: 14.2 kDa), and also immunoglobulins (MW light chain: 25 kDa; MW heavy chain: 50 kDa), bovine serum albumin (MW: 66.3 kDa), bovine lactoferrin (MW: 80 kDa), lactoperoxidase (MW: 70 kDa), and other minor proteins as glycomacropeptide (MW: 6.7 kDa) (Madureira et al., 2007; Phillips & Williams, 2011). A fundamental drawback of WPI is its sensitivity to changes in pH and ionic strength, and thermal treatments which restrict their application in some products (Ahmad et al., 2020; Bédié et al., 2008; Wagoner & Foegeding, 2017).

One strategy to overcome these limitations is the formation of complexes by electrostatic assembly with polysaccharides with an opposite net charge to WPI. Different phase behavior can arise when aqueous suspensions of proteins and polysaccharides are mixed (Gaber et al., 2018; Goh et al., 2019; Kong et al., 2022). If the polymers are incompatible, co-solubility of biopolymers or thermodynamic incompatibility (segregation) can occur. The incompatibility typically occurs when the biopolymers have the same charge (either negative or positive net charge) and electrostatic repulsive interactions are strong. On the other way, if the polymers are compatible, soluble complexes or insoluble complexes (coacervates) can be formed. Compatibility usually occurs when the biopolymers have opposed net charges to accept attractive interactions. Besides, compatibility appears at low biopolymer concentrations (Gaber et al., 2018; Goh et al., 2019). In addition, several factors determine the protein-polysaccharide interactions and complex formation, including biopolymer characteristics (molecular weight, molecular con-

* Corresponding author at: Departamento de Ciencia y Tecnología, Laboratorio de Investigación en Funcionalidad y Tecnología de Alimentos (LIFTA), Universidad Nacional de Quilmes, Roque Sáenz Peña 352, B1876BXD, Bernal, Buenos Aires, Argentina.
E-mail address: gonzalo.palazolo@unq.edu.ar (G.G. Palazolo).

https://doi.org/10.1016/j.focha.2022.100123
Received 21 April 2022; Received in revised form 5 September 2022; Accepted 18 October 2022

formation, charge density, and rigidity), environmental conditions (pH and ionic strength), biopolymer ratio, biopolymer total concentration, and additional treatments (heat or mechanical treatments) (Behrouzain & Razavi, 2020; Devi et al., 2017). The pH is the main factor affecting the formation of complexes since, for the electrostatic assembly, both protein and polysaccharide should bear opposite surface charges. The ionic strength is the second factor determining the formation and characteristics of protein-polysaccharide complexes. However, its effect is difficult to predict since it depends both on the type of salt and the characteristics of the proteins and polysaccharides. In general, the addition of monovalent ions (such as Na^+ or Cl^-) could neutralize groups with negative and positive charges that in other conditions would interact with each other, disadvantaging the formation of complexes and favoring the hydration of each polymer. However, in higher salt concentrations, the monovalent ions could interact with the water, dehydrating the biopolymers and inducing protein-protein and protein-polysaccharide interactions. Finally, the protein:polysaccharide ratio and total biopolymer concentration also affect the formation and characteristics of electrostatic complexes. The literature shows that the better stoichiometric protein:polysaccharide ratio depends mainly on the biopolymers' charge density, conformation, and flexibility (Gaber et al., 2018; Jones & McClements, 2011; Lan et al., 2020b).

Soluble soybean polysaccharides (SSPS) are a by-product of industries producing tofu, soy milk, and soy protein. Specifically, SSPS are a family of pectin-like acidic biopolymers used as dietary fiber and as a functional ingredient because of their nutritional value and benefits as lowering blood cholesterol and reducing diabetes risk (Chen et al., 2010; Jia et al., 2015; Maeda & Nakamura, 2009). SSPS is composed of a main rhamnogalacturonan backbone branched by β-1,4−galactan and α−1,3− or α−1,5−arabinan chains. In addition, the polysaccharide chain has associated protein moieties which apport interesting characteristics to this biopolymer and could facilitate the complexation between protein and polysaccharide (Li et al., 2020; Nakamura et al., 2004). SSPS have high water solubility, low bulk viscosity, low pH, and high-temperature stability (Maeda & Nakamura, 2009; Xu & Liu, 2016).

Many studies have been conducted on the interaction of WPI with different polysaccharides, including pectin (Chanasattru et al., 2009; Gentés et al., 2010), alginate (Fioramonti et al., 2014), gum arabic (Weinbreck et al., 2004a, 2004b), carrageenan (Weinbreck et al., 2004c), flaxseed gum (Liu et al., 2020a), basil seed gum (Behrouzain et al., 2020; Behrouzain & Razavi, 2020), hyaluronic acid (Zhong et al., 2021), quince seed mucilage (Ghadermazi et al., 2019a, 2020b), and *Tremella fuciformis* polysaccharide (Hu et al., 2019). However, as far as we are aware, only two previous studies analyzed the interaction between WPI and SSPS. In our previous work, we studied the effect of heat-treatment on the complex formation at pH 3.5 and 4:6 WPI:SSPS ratio, comparing single- and two-step assembly approaches for application in emulsions subjected to freeze-thawing (Cabezas et al., 2019). Recently, Zamani et al. (2020) employed WPI-SSPS mixtures obtained at pH 7.0 and 3.5 with or without heat treatment for WPI stabilization in beverages. However, the effects of other parameters in the complexation process were not further characterized. So, the interaction between SSPS and WPI has not been thoroughly characterized and WPI-SSPS mixtures are still not used in the food industry since there is a lack of fundamental understanding of physical and chemical interactions between these biopolymers.

Hence, the main objectives of the present work were to determine the pH, WPI:SSPS mass ratio, and NaCl-added concentration conditions that allow the complexes' formation from WPI and SSPS, and to characterize the size, charge, and physical stability of the obtained WPI-SSPS complexes. The knowledge generated in this work is useful to design WPI-SSPS complexes with specific characteristics of size, charge, and physical stability. The possibility of modifying their characteristics would allow the incorporation and use of these complexes in food, medicinal or cosmetic matrices for different purposes. Concerning their specific applicability in Food Science, WPI-SSPS complexes could be used for the encapsulation and delivery of bioactive compounds, the stabilization of emulsions and foams, or the modification of optical and rheological properties of the food matrix. However, the novel and improved functionality of these WPI-SSPS complexes concerning WPI control must still be studied.

2. Materials and methods

2.1. Materials

Arla Foods Ingredients Argentina, S.A (Buenos Aires, Argentina) donated the whey protein isolate (WPI, Lacprodan® DI-9224). According to the supplier's datasheet, the WPI chemical composition (% w/w) was: crude protein (N × 6.25), 86.5; lactose, 0.1; total fat, 0.1; salts, 1.25. Fuji Oil Co. Ltd (Osaka, Japan) donated the soluble soybean polysaccharides (SSPS, Soyafibe-SCA100). According to the supplier's datasheet, the SSPS chemical composition (% w/w) was: total dietary fiber, 75.1; crude protein (N × 6.25), 7.8; moisture, 5.8; ash, 7.8. Besides, the SSPS saccharide composition (% w/w) was: rhamnose, 5.0; fucose, 3.2; rabinose, 22.6; xylose, 3.7; galactose, 46.1; glucose, 1.2; and galacturonic acid, 18.2. The three SSPS majority components had molecular weights of 550 kDa, 25 kDa, and 5 kDa, respectively (Maeda & Nakamura, 2009). WPI and SSPS powders were utilized with no further purification. Deionized water was used to prepare the solutions and dispersions. All the other chemicals were analytical-grade reagents purchased from local distributors (Buenos Aires, Argentina).

2.2. Preparation of protein and polysaccharide stock dispersions

Using a calibrated Ohaus® Pioneer® PA214 analytical balance (resolution ± 0.0001 g) the solid powders of WPI and SSPS were weighted and mixed into deionized water under constant mixing for 2 h at room temperature (25 ± 2 °C) to prepare a 4% w/w WPI and SSPS stock solution dispersion. The pH values of WPI and SSPS stock dispersions were 7.00 ± 0.02, and 5.80 ± 0.04, respectively. To prevent microbial growth, sodium azide at a final concentration of 0.02 % w/w was added to all dispersions, which were further stored at room temperature, protected from light, until use.

2.3. Preparation and characterization of protein-polysaccharide mixtures

2.3.1. Preparation of protein-polysaccharide mixtures

To prepare binary mixtures with desired mass ratios (1:1, 2:1, 4:1, 6:1, 8:1, or 10:1 WPI:SSPS), appropriate proportions of the two stocks dispersions were mixed with a magnetic stirrer for 1 h at room temperature (25 ± 2 °C). The binary mixtures were prepared with deionized water or with concentrated NaCl solutions to assure the desired final NaCl-added concentration (0, 50, or 100 mM NaCl). Then, the pH of each mixture was adjusted with 1.0 M HCl to desired pH (7.0, 6.5, 6.0, 5.5, 5.0, 4.5, 4.0, 3.5, 3.0, 2.5, or 2.0). pH was measured using a C861 Consort pH/mV meter with a PY-P10-25 Sartorius electrode (resolution ± 0.01), calibrated daily before use. The final WPI concentration was 1.0 % w/w in all the dispersions, and the SSPS concentrations varied between 1.0 and 0.1 % w/w. Individual 1.0 % w/w WPI and SSPS dispersions were used as control samples.

2.3.2. ζ-potential determination

The ζ-potential of individual biopolymer dispersions was determined at 25 ± 2 °C with a Zetasizer Nano ZSP ZEN 5600 analyzer (Malvern Instrument, UK) at pH values between 7.0 and 2.5. In addition, the ζ-potential of the 4:1 WPI:SSPS mixture was determined in the same pH range. The refractive indices were 1.54 and 1.33 for biopolymers (WPI, SSPS, and WPI-SSPS mixture) and dispersant, respectively. For measurements, dispersions were diluted (1:3 v/v) with deionized water previously adjusted at each pH with HCl 1.0 M, to avoid multiple light scattering effects. The dilutions were performed using calibrated Gilson® automatic pipettes.

2.3.3. Turbidimetric analysis and calculation of critical pH

The turbidity of WPI, SSPS, and WPI-SSPS mixtures at different pH, WPI:SSPS ratio, and NaCl-added concentrations was expressed as the apparent optical density at 600 nm using a Biochrom Libra S4 visible spectrophotometer (Biochrom Instruments; United Kingdom). All measurements were conducted at room temperature (25 ± 2 °C).

From the parameterization of the turbidity results as a function of pH, the critical pH values were calculated as elsewhere (Behrouzain & Razavi, 2020; Liu et al., 2009; Zhong et al., 2021). The pH where occurs the maximum complex formation (pH_{opt}) was determined at the maximum optical density at 600 nm. The pH where start the formation of intramolecular soluble complexes (pH_c) was determined as a slight increase in scattered light intensity. The pH where begin the formation of intramolecular insoluble complexes ($pH_{\varphi 1}$) was determined by extending tangent lines on both sides of the inflection point at pH higher than pH_{opt}. Finally, the pH where start the disassembly of complexes ($pH_{\varphi 2}$) was determined by extending tangent lines on both sides of the inflection point at pH lower than $pH_{opt.}$

2.3.4. Construction of state diagrams

The physical dispersion state of WPI, SSPS, and WPI-SSPS mixtures at different pH, WPI:SSPS ratio, and NaCl-added concentrations was analyzed by visual observation on days 1 and 14 post-production (Lan et al., 2018a, 2020b). Each day, the samples were classified into five groups based on the turbidity of the suspension and the presence/absence of precipitate (Fig. S1). The samples were statically stored upright at room temperature (25 ± 2 °C) and protected from light during the study.

2.4. Preparation and characterization of protein-polysaccharide complexes

2.4.1. Preparation of protein-polysaccharide complexes

From the analysis of the results obtained so far, the conditions that allow obtaining insoluble (sedimentable and non-sedimentable) complexes were selected. Specifically, three pH conditions (4.0, 3.5, and 3.0), three WPI:SSPS mass ratios (2:1, 4:1, and 6:1), and three NaCl-added concentrations (0, 50, and 100 mM) were chosen to continue the characterization. As in Section 2.3.1, the WPI-SSPS soluble complexes were obtained by mixing appropriate proportions of both biopolymers stock dispersion with deionized water or concentrated NaCl solution with a magnetic stirrer for 1 h at room temperature (25 ± 2 °C), to obtain the desired mixing WPI:SSPS mass ratios and salt concentrations. Then, the pH of each mixture was adjusted with 1.0 M HCl to the desired pH. The final WPI concentration was 1.0 % w/w in all the dispersions and the SSPS concentrations varied between 0.50 and 0.17% w/w. Individual WPI and SSPS dispersions were used as control samples.

2.4.2. ζ-Potential determination

The ζ-potentials of WPI, SSPS, or WPI-SSPS complexes were determined as previously explained in Section 2.3.2.

2.4.3. Particle size measurements

The particle size distribution (PSD), hydrodynamic diameter (Z-average, intensity weighted average diameter), and polydispersity index (PDI) of WPI, SSPS, or WPI-SSPS complexes were determined at 25 ± 2 °C by dynamic light scattering using a Zetasizer Nano ZAP ZEN 5600 analyzer (Malvern Instruments, UK). To avoid multiple light scattering effects, samples were diluted (1:3 v/v) with deionized water previously adjusted at specific pH with HCl 1.0 M. The refractive indices for the complexes and dispersant were 1.54 and 1.33, respectively. The Z-average and PDI were determined on days 0, 28, and 56 post-production.

2.4.4. Physical stability

The physical stability of WPI, SSPS, or WPI-SSPS complexes' dispersions was monitored using a Turbiscan Lab® vertical analyzer (Formulaction, France), according to the multiple light scattering theory. For measurements, all samples were transferred into cylindrical glass tubes, and the transmission (T) and backscattering (BS) throughout the entire sample were determined up to day 56 post-production. The samples were statically stored at room temperature (25 ± 2 °C) and protected from light during the study. The stability of the complexes was evaluated from the T and BS profiles and the global Turbiscan stability index (TSI), calculated by TurbiSoft software (Formulaction, France).

2.5. Statistical analysis

All the preparations and characterization assays were conducted at least in triplicate and the results were expressed as mean ± standard deviation. The statistical analyses were performed using Graph Pad Prism v6.0. One-way ANOVA or Two-way ANOVA followed by multiple comparisons post-test were used depending on the experimental design. The differences were considered significant only when the p-value was less than 0.05. Furthermore, in the characterization of WPI-SSPS complexes, the effects of the three independent variables (pH, WPI:SSPS mass ratio, and NaCl-added concentration) on the Z-average, ζ-potential, and TSI of WPI-SSPS complexes were examined by a 3 × 3 factorial design for the response surface and mesh methodology by Statgraphics Centurion XVI v16.1.18.

3. Results and discussion

3.1. Characterization of protein-polysaccharide mixtures

3.1.1. ζ-potential analyses

The ζ-potentials of individual biopolymer dispersions and the 4:1 WPI:SSPS mixture at pH values between 7.0 and 2.5 were determined to understand the driving force for electrostatic interactions (Fig. 1).

The WPI control presented ζ-potential varying between +22.2 ± 1.4 mV at pH 2.5 to -27.9 ± 0.9 mV at pH 7.0 (Fig. 1A), with the isoelectric point (pI) occurring at 4.3. This result agrees with previous works that reported a WPI pI of 4.3–4.5 (Behrouzain & Razavi, 2020; Yi et al., 2021; Zhong et al., 2021). In addition to the change in ζ-potential values, the precipitation of WPI at pH ranging from 5.0 to 3.5 was observed (Fig. 1B). This precipitation of protein aggregates is mediated by the lack of electrostatic repulsion and becomes one of the major challenges to WPI incorporation in acidic foods (Hu et al., 2019).

On the other hand, the SSPS control presented negative ζ-potentials in the entire pH range, varying from -0.9 ± 0.1 mV at pH 2.5 to –21.5 ± 0.6 mV at pH 5.5, indicating a pKa < 2.5 (Fig. 1A). These results are consistent with those previously reported (Zhao et al., 2018) and with the presence of galacturonic acid as a component sugar of this polysaccharide. Moreover, SSPS control formed stable translucent dispersions throughout the studied pH range (Fig. 1 B).

According to these results, WPI and SSPS would be compatible at 2.5 < pH < 4.3 since complexes are formed by the electrostatic attraction of biopolymers with opposite net charges. In this work, the biopolymer interaction and formation of the WPI-SSPS complexes were confirmed by the change in the ζ-potential of the 4:1 WPI:SSPS mixture concerning the WPI and SSPS controls (Fig. 1 A) and by the formation of stable dispersions in pH close to WPI pI (Fig. 1 B). At this WPI:SSPS ratio, the complexes presented a pI value close to 3.8.

3.1.2. Turbidimetry analysis

Turbidimetry analysis was performed to examine the effects of pH (7.0 to 2.0), WPI:SSPS mass ratio (1:1 to 10:1), and NaCl concentration (0, 50, or 100 mM NaCl) on the WPI-SSPS interactions (Fig. 2).

The WPI controls presented different turbidity and tendency to precipitate as a function of pH and NaCl concentration. In the absence of added salt, a marked increase in WPI turbidity in pH close to the pI was observed (Fig. 2A) on day 0 of preparation, which corresponds to the formation of large-size protein aggregates with high light-scattering capacity. This maximum turbidity was attributed to relatively weak

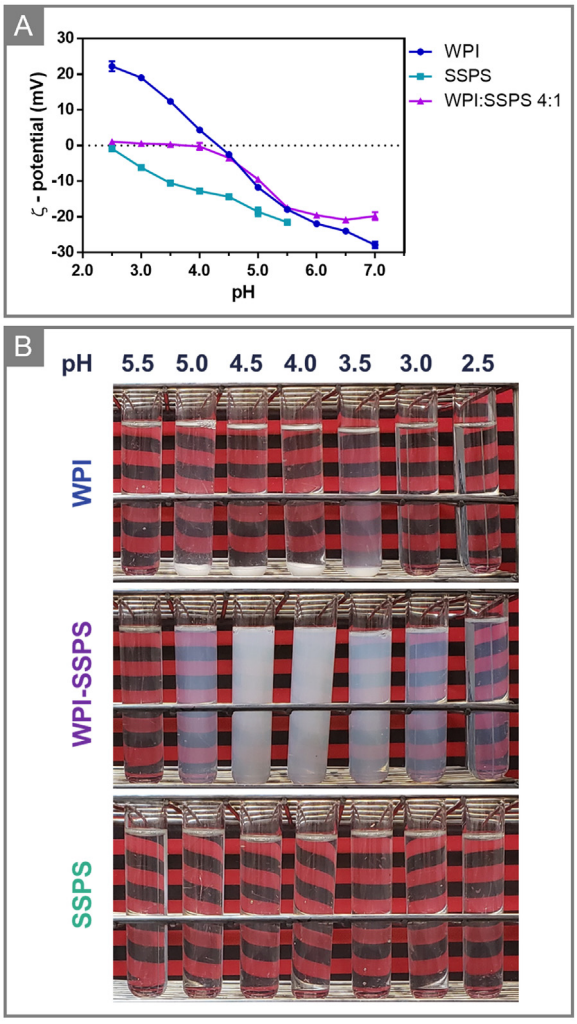

Fig. 1. (A) ζ-potential of WPI, SSPS, and mixture at 4:1 WPI:SSPS ratio as a function of pH. (B) Photographs of WPI, SSPS, and mixture at 4:1 WPI:SSPS ratio as a function of pH on day 1 post-production.

electrostatic repulsion between protein molecules leading to WPI self-association (Behrouzain et al., 2020). On day 1 post-preparation, WPI precipitated and formed translucent dispersion in pH ranging from 5.0 to 4.0 (Fig. S2A), which corresponds with the extensive protein aggregation (Zhong et al., 2021). On the contrary, in the presence of 50 and 100 mM of NaCl, the WPI turbidity significantly decreased compared to the case without added salt (Fig. 2 A). This trend could be explained by the formation of smaller-size protein aggregates or the formation of fewer quantities of protein aggregates. On day 1 post-production, WPI in presence of 50 and 100 mM NaCl also precipitated in pH between 5.0 and 3.5, but the suspension remained appreciably cloudy (Fig. S2A). As explained before, this phenomenon is defined by a salting-in effect or by the formation of smaller non-sedimentable protein aggregates.

On the other hand, the SSPS controls generated translucent dispersions (Fig. S2B) with low turbidity (Fig. 2A) in the entire pH range and salt concentrations.

The WPI-SSPS mixtures presented, as WPI, different turbidity trends and tend to precipitate as a function of pH and salt concentration. In absence of added salt, the mixtures with different WPI:SSPS ratios gave rise to a decrease in turbidity compared to the WPI control in pH close to pI (Figs. 2 A and S3), which could be due to the formation of protein-polysaccharide complexes with smaller sizes and light-scattering capacity than protein aggregates. Besides, as the available SSPS increased and WPI:SSPS ratio decreased (from 10:1 to 1:1), a shift in the turbidity maximum toward lower pH was observed (Fig. 2A). This observation means that the pH value should be reduced to promote the optimal neutralization of all the WPI positive charges by the anionic groups of SSPS (Ghadermazi et al., 2019a, 2020b). Klemmer et al. (2012) observed a similar trend for mixtures of pea protein isolate and alginate with protein:polysaccharide mass ratio between 20:1 to 1:1. On day 1 post-production, no precipitation was observed in any pH conditions (Fig. S3). This result confirmed the formation of non-sedimentable electrostatic complexes in 2.5 < pH < 4.3 conditions, without added salt, for all the WPI:SSPS mass ratios. On the contrary, in the presence of 50 and 100 mM of NaCl, most of the mixtures presented higher turbidity than the WPI control (Figs. 2 A, S4, and S5), which is explained by the formation of smaller protein aggregates in WPI control and larger complexes in WPI-SSPS mixtures. Likewise, the WPI-SSPS mixtures in presence of 50 and 100 mM of NaCl presented higher turbidity than WPI-SSPS mixtures without salt added (Fig. 2A), which could be due to the formation of larger-size complexes in presence of salt. Specifically, it was observed that the turbidity of the samples significantly in-

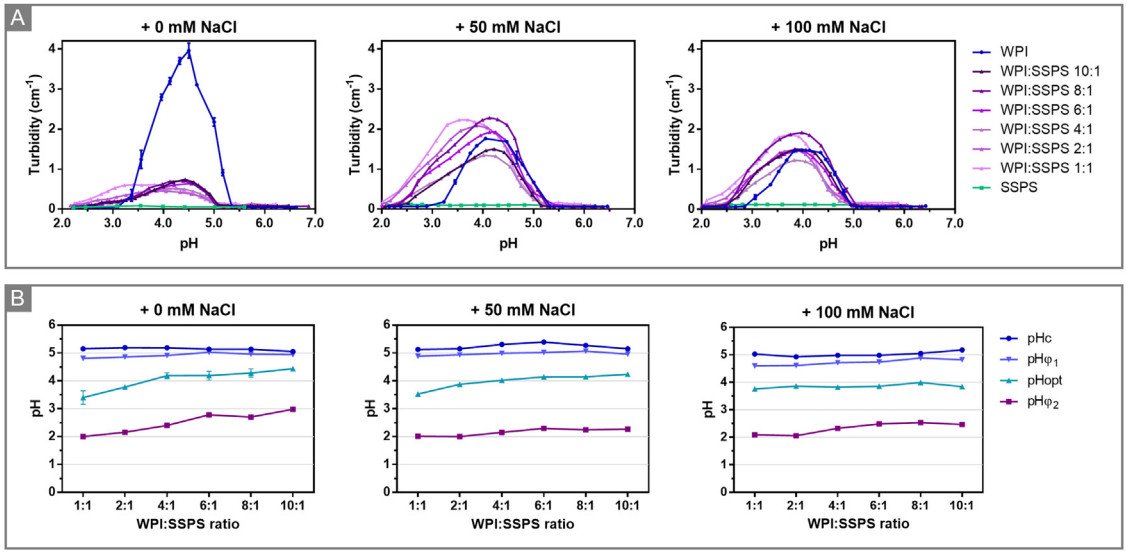

Fig. 2. (A) Turbidity of WPI, SSPS, or mixtures at different WPI:SSPS ratios as a function of pH and NaCl-added concentration. (B) Critical pH values as a function of WPI:SSPS ratio and NaCl-added concentration.

creased with the increment in NaCl concentration from 0 to 50 mM, but then the turbidity slightly decreased with the increment up to 100 mM. Bastos et al. (2018) reported the same tendency for lactoferrin-alginate mixtures in presence of 0–200 mM of NaCl-added concentrations. On day 1 post-production, precipitation was observed for 6:1 and 8:1 WPI:SPPS mixtures at pH 5.0 in presence of 100 mM NaCl, and no precipitation was observed in the rest of the samples (Figs. S4 and S5). In general, as the salt concentration increased, the dispersions became cloudier and unstable. These observations could be explained by the interaction of NaCl ions with both biopolymers. Monovalent anions, like chloride, bind to positive groups in the proteins, altering their general charge characteristics. In the same way, sodium ions may interact with negative groups in the protein chains, but it is reported that they do not have as significant an effect as anions (Damodaran et al., 2007). The interaction of Na^+ and Cl^- with biopolymers might form a double layer of ionic groups, which decreases the electrostatic interaction between both protein molecules and protein-polysaccharide molecules (Bastos et al., 2018; Stone & Nickerson, 2012). Moreover, these interactions cause more solvation of proteins and, thus, increase their solubility. However, at high salt concentrations, most water molecules are strongly bound to salt ions, and the reorganization of water molecules around biopolymers occurs. This could result in stronger protein-protein and protein-polysaccharide interactions, which could explain the formation of larger particles with higher turbidity in WPI-SSPS mixtures in presence of 50 and 100 mM of NaCl. Nevertheless, these effects must be carefully analyzed since depends on the type of protein and polysaccharide. For example, Stone & Nickerson (2012) reported that the complexation of WPI with both ι- and λ-carrageenan types was enhanced up to 300 mM of NaCl, while the complexation of WPI with κ-carrageenan type was decremented with the addition of salt.

3.1.3. Critical pH values

From the parameterization of the turbidimetry results, the critical pH values were calculated (Fig. 2 B), including the pH at soluble complexes begin to form (pH_c), the pH at insoluble complexes begin to form ($pH_{\varphi 1}$), the optimum pH for complex formation (pH_{opt}), and the pH at the complexes disassemble ($pH_{\varphi 2}$). Independently of WPI:SSPS ratio and salt concentration, all trends were characterized by four different regions by pH decreasing.

In the first region, where $pH > pH_c$, the WPI and SPPS presumably coexist as cosoluble individual molecules due to steric hindrance and electrostatic repulsion between the strongly negatively charge biopolymers (incompatibility), resulting in translucent dispersions. Non-significant differences were obtained in the pH_c for any WPI:SSPS ratio or NaCl concentration ($p > 0.05$).

In the second region, where $pH_c > pH > pH_{\varphi 1}$, the WPI and SPPS interact with each other forming intramolecular soluble WPI-SSPS complexes. This could happen above the pI of WPI since SSPS can bind to positive patches on the protein surface, even though both the protein and polysaccharide have a net negative charge (Behrouzain et al., 2020; Jones et al., 2010; Stone & Nickerson, 2012). Hadian et al. (2016) showed that interactions at pH > pI of protein were possible in mixtures of β-lactoglobulin and the water-soluble fraction of Persian gum. Non-significant differences were obtained in the $pH_{\varphi 1}$ for any WPI:SSPS ratio; but significant differences ($p < 0.01$) were observed for $pH_{\varphi 1}$ of 1:1 and 2:1 WPI:SSPS mixtures when NaCl concentration increased from 0 to 100 mM. Liu et al., 2020a reported similar results for WPI and flaxseed gum mixtures with increasing NaCl concentration from 0 to 50 mM.

In the third region, where $pH_{\varphi 1} > pH > pH_{\varphi 2}$, going through the pH_{opt}, the WPI and SSPS interact with each other forming WPI-SSPS insoluble complexes that can sediment or not sediment depending on their particle size (Gaber et al., 2018). In the present work, sedimentation of complexes was observed only in the higher salt concentration, but non-sedimentable complexes were obtained in the rest of the conditions, which could be related to the formation of nanosized complexes. It has been reported that complexes could grow in size in a fractal manner as the pH declines (Rodriguez Patino & Pilosof, 2011; Stone & Nickerson, 2012) since the protein assumes a more positive charge that allows the nucleation and growth-type kinetic mechanism (Girard et al., 2004) until equimolar quantities between the two polymers are achieved and evidenced a maximum in scattering intensity (pH_{opt}). Beyond this pH_{opt}, scattering declines because the anionic groups of the polysaccharide chain become protonated leading to fewer biopolymer interactions and complete dissociation of structure (Sanchez et al., 2006). Besides electrostatic interactions, the hydrogen bond, hydrophobic interactions, and van der Waals interactions also play a role in the interaction of the protein and polysaccharide (Gentile, 2020). However, electrostatic interactions play the dominant role in molecular (Cortés-Morales et al., 2021; Li et al., 2022).

In this third region could also be observed that the pH range in which electrostatic complexes are formed (range between pH_c and $pH_{\varphi 2}$) was widened as the WPI:SSPS ratio decreased from 10:1 to 1:1, because $pH_{\varphi 2}$ decreased from 3.0 in the ratio 10:1 to 2.5 in the ratio 1:1. Both pH_{opt} and $pH_{\varphi 2}$ presented significant differences ($p < 0.05$) for mixtures obtained at 1:1, 2:1, 4:1, and 6:1 WPI:SSPS ratios, however, non-significant differences were observed for these parameters in 6:1, 8:1 and 10:1 WPI:SSPS ratios. This phenomenon is probably associated with a greater tendency to charge neutralization in WPI-SSPS mixtures when more SSPS was available (Fioramonti et al., 2014). The same trend between critical pH values and protein:polysaccharide mixing ratio has been previously reported for different biopolymers systems. Lan et al. (2018a) observed this trend for the interaction of pea protein isolation with high methoxy pectin in ratios from 20:1 to 1:1 (i.e., pectin concentration increased), while Fioramonti et al. (2014) reported this trend for the interaction of WPI with alginate in ratios from 6:1 to 2:1 (i.e., alginate concentration increased). In the same way, Azarikia & Abbasi (2016) reported this tendency for the interaction of WPI with the soluble fraction of gum tragacanth and the soluble fraction of Persian gum, while Hadian et al. (2016) reported this tendency for β-lactoglobulin and soluble fraction of Persian gum. Besides, by increasing the salt concentration, the pH range in which electrostatic complexes are formed was extended. This could occur because the ions provided by the salt could neutralize certain charges of the biopolymers, inducing the interaction of more hydrophobic zones, as we explained previously. Zhang et al. (2021) reported parallel results for the effect of NaCl concentration on critical pH values of field pea protein isolate with chitosan. Hadian et al. (2016) showed similar results for the effect of both NaCl and $CaCl_2$ on critical pH values of β-lactoglobulin and the water-soluble fraction of Persian gum.

In the fourth region, at $pH < pH_{\varphi 2}$, the complexes disassemble probably due to the loss of charge of the SSPS molecules that reach the pKa of their carboxylic groups (Bédié et al., 2008). The $pH_{\varphi 2}$ was observed to be declined towards a lower pH value with the reduction of the WPI:SSPS ratio (from 10:1 to 1:1), which could be due to the stronger interconnected network at higher SSPS availability (Zhong et al., 2021).

3.1.4. State diagram

The state diagrams were constructed from the macroscopic observation of the dispersions throughout the storage time (Figs. 3 and S1). The WPI showed precipitation in pH ranging from 5.0 to 4.0 on day 1 post-preparation, which corresponds with the extensive protein aggregation due to lack of repulsion since pH is close to pI. While in the absence of salt the suspension was translucent, in the presence of 50 and 100 mM NaCl the suspension remained appreciably cloudy, which could be due to a salting-in effect or by the formation of smaller non-sedimentable protein aggregates. These results are in concordance with those obtained and discussed for turbidity measurements (Section 3.1.2). Moreover, the WPI controls with 0 or 50 mM of NaCl did not present changes along the 14 days, whereas the WPI controls with 100 mM of NaCl changed from cloudy to translucent suspensions, both with precipitate, between days 1 and 14. This phenomenon showed that, even at high salt concen-

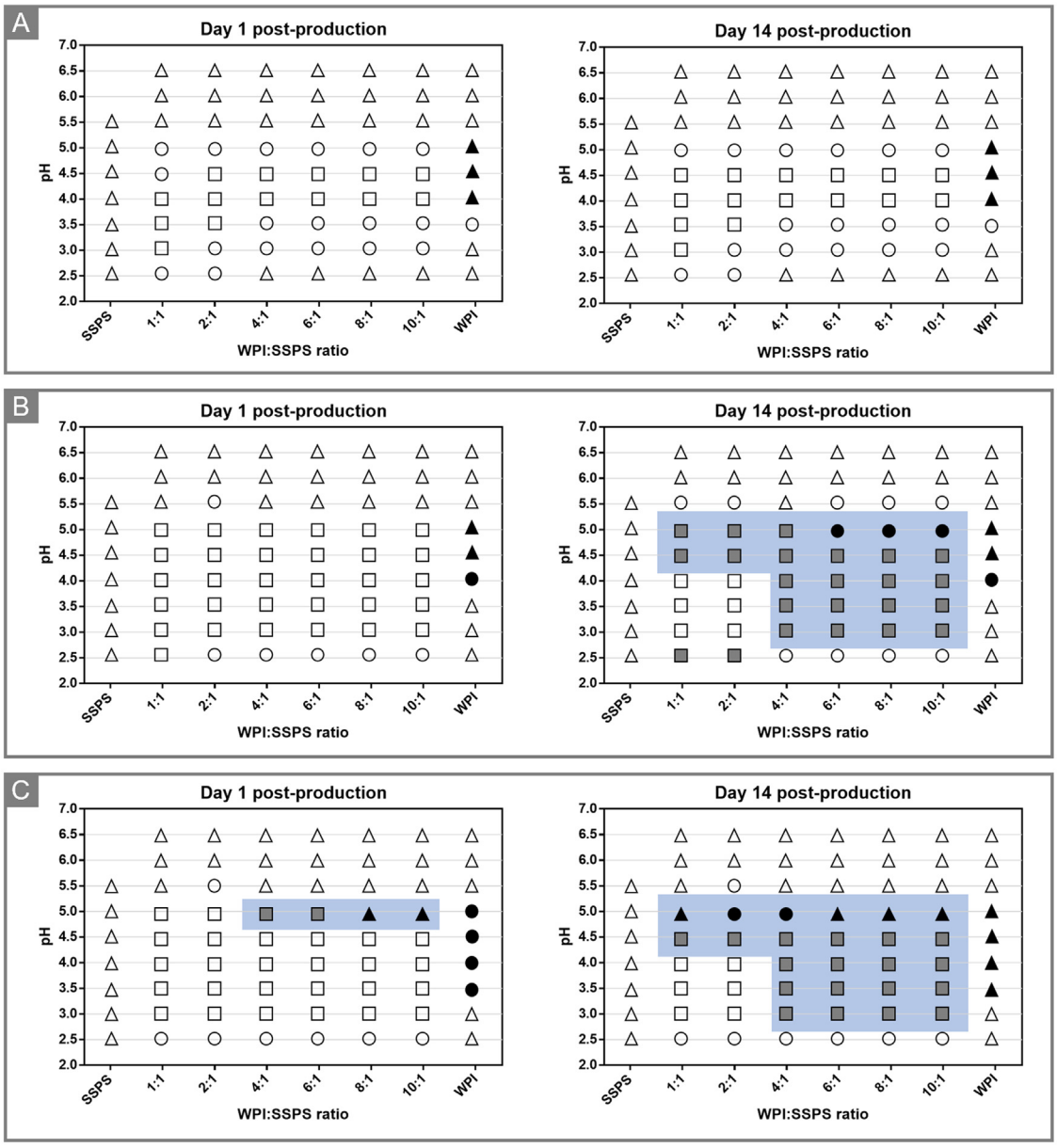

Fig. 3. State diagram of WPI, SSPS, and mixtures at different WPI:SSPS ratios as function of pH and (A) 0 mM, (B) 50 mM, or (C) 100 mM NaCl-added concentration. The state corresponds to translucent suspension (△), cloudy suspension (○), high turbidity suspension (□), clarification without precipitate (■), precipitate with cloudy suspension (●), or precipitate with translucent suspension (▲).

trations, WPI is unstable at a pH close to its pI. On the other hand, the SSPS control maintained its stability across the storage period.

Concerning the WPI-SSPS mixtures, the samples were translucent at pH > pHc (pH > 5.5), which could be due to the negative charge of both biopolymers leading to electrostatic repulsion (incompatibility). On the contrary, different phase behaviors were observed in pH < pHc (pH < 5.5) when protein-polysaccharide complexes could be formed (compatibility). Mixtures obtained without NaCl (Fig. 3A) were stable between day 1 and 14 post-production. Regarding the effect of NaCl concentration on day 1 post-production, the mixtures with 100 mM were cloudier than the samples obtained in 50 mM NaCl, and those were cloudier than the samples obtained without added salt. These results are in harmony with those obtained for turbidity measurements (Section 3.1.2) and are related to the possible increment of complexes' size induced by NaCl concentration, as previously discussed. In addition, the 4:1 to 10:1 WPI:SSPS mixtures obtained at pH 5.0 in 100 mM of NaCl exhibited rapid destabilization and clarification with or without precipitation. These results are consistent with the formation of unstable larger complexes and protein-aggregates, which could happen because the pH is not yet close to the pH_{opt} for WPI-SSPS interaction and because the concentration of SSPS is not enough to increase the stability of the WPI. On day 14 post-production, only the 1:1 and 2:1 WPI:SSPS mixtures obtained at pH 3.0–4.0 remained stable, while the remaining samples were unstable in the presence of 50 and 100 mM NaCl. Specifically, the samples at pH < 4.5 presented clarification without precipitation which could be due to the slow sedimentation of larger complexes obtained in presence of salt as we discussed earlier. On the other hand, the samples at pH = 5,0 showed sedimentation and precipitation which could be explained by the distance with the pH_{opt} and the low SSPS concentration. About this, as the available SSPS increased and WPI:SSPS ratio decreased (from 10:1 to 1:1), the complexes became more stable hypothetically because they had a smaller particle size. Azarikia & Abbasi (2016) reported similar phase behavior for mixtures of WPI with the soluble fraction of gum tragacanth and Persian gum; as the avail-

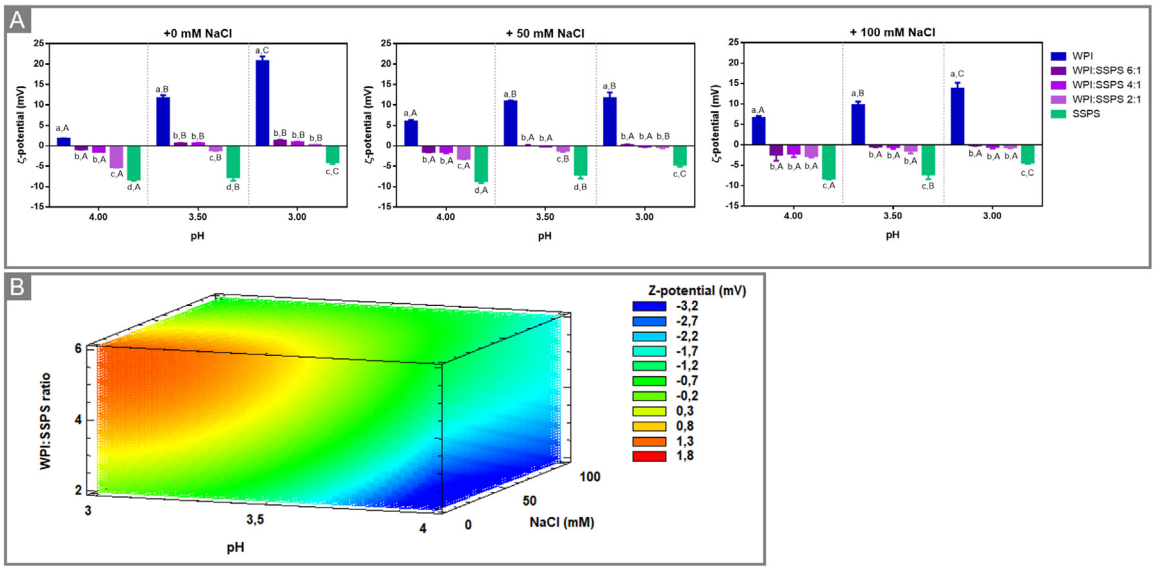

Fig. 4. (A) ζ-potential of WPI, SSPS, or complexes at different WPI:SSPS ratios as a function of pH and NaCl-added concentration. Different lowercase letters indicate significant differences ($p < 0.05$) between different samples at the same pH condition. Different uppercase letters indicate significant differences ($p < 0.05$) between the same sample at different pH conditions. (B) Statistical response mesh for ζ-potential as a function of pH, WPI:SSPS ratio, and NaCl-added concentration.

ability of polysaccharides increased, the complexes became more stable showing no precipitation. Besides, Zhong et al. (2021) described similar phase behavior for mixtures of WPI with hyaluronic acid (HA); where WPI:HA mass ratio lower than 4:1 showed no precipitation and mixtures with WPI:HA ratio of 4:1 or higher showed precipitation and destabilization.

3.1.5. Conditions for protein-polysaccharide complexes obtention

From the results obtained so far, the conditions to assure the obtention of insoluble (sedimentable and non-sedimentable) complexes were selected. Specifically, it was decided to continue working with pH conditions of 4.0, 3.5, and 3.0, since WPI-SSPS attractive electrostatic interactions are ensured in that range (compatibility situation), as can be seen in the results of ζ-potential (Fig. 1) and through turbidimetry (Fig. 2). In addition, the 2:1, 4:1, and 6:1 WPI:SSPS mass ratios were selected because changes in the critical pH values (Fig. 2) and the storage stability by state diagram (Fig. 3) were observed in these mass ratios. Finally, it was decided to continue working with the three salt-added concentrations because appreciable changes were noticed in the critical pH values (Fig. 2) and the storage stability (Fig. 3). The characteristics of WPI-SSPS complexes were analyzed in Section 3.2 to deeply understand the effects of the selected pH, WPI:SSPS mass ratio, and NaCl-added concentration.

3.2. Characterization of protein-polysaccharide complexes

The WPI-SSPS complexes obtained in the selected conditions were characterized by ζ-potential (Fig. 4A), Z-average (Fig. 5A), polydispersity index (PDI, Fig. 5B), and physical stability overtime followed by Turbiscan stability index (TSI, Fig. 6A–C). Moreover, from the obtained experimental results, the statistical response meshes (Figs. 4B, 5C, and 6D) and surfaces (Figs. S6, S7, and S9) were calculated, as well as the influence of each parameter (pH, WPI:SSPS ratio, and NaCl concentration) in the main characteristics of the complexes (ζ-potential, Z-average, and TSI).

3.2.1. ζ-Potential

According to ζ-potential measurements (Fig. 4A), as expected, a net positive charge was observed in the WPI controls. The ζ-potential module of WPI significantly increased ($p < 0.01$) as the pH moved away from the pI because of the neutralization of negatively charged groups. On the other hand, the ζ-potential module of WPI decreased as the salt concentration increased (from 0 to 100 mM of NaCl) since chloride ions neutralized positively charged groups of proteins more effectively than sodium ions neutralized negatively charged groups (Damodaran et al., 2007). On the other hand, a net negative charge was observed in the SSPS control, whose module significantly reduced ($p < 0.05$) as the pH moved close to the pKa. The NaCl concentration did not significantly modify the ζ-potential of SSPS ($p > 0.05$). The complementary net charges allow the WPI-SSPS complexes formation that presented ζ-potential values around zero. ζ-potential values indicate that the strongest WPI-SSPS interactions showed in spectrophotometry occurred when the electrical charge of the mixtures was nearly neutralized. However, it is important to note that the ζ-potential of the mixtures represents the net ζ-potential value of protein-polysaccharide complexes and non-interacting individual biopolymers (Gorji et al., 2018).

According to the statistical response mesh (Fig. 4B) and surfaces (Fig. S6), the pH, WPI:SSPS ratio, and NaCl concentration, and also the interaction between these parameters, had a significant effect on the ζ-potential of complexes. As the pH increases (from 3.0 to 4.0), the ζ-potential of WPI-SSPS complexes becomes more negative. This could be due to the proteins contribute with a smaller amount of positive charge, so the negative charge of SSPS is not completely neutralized, giving rise to complexes with a negative surface charge. Gorji et al. (2018) reported a similar trend for mixtures of β-lactoglobulin or α-lactalbumin with alginate, where the ζ-potential values decreased with the increasing pH. On the other hand, as the WPI:SSPS ratio decreased (from 6:1 to 2:1), the negative charge increased, which could be due to a greater amount of SSPS available to neutralize the positive charge of the proteins. This result agrees with those obtained by Zhong et al. (2021), who studied the ζ-potential of WPI-hyaluronic acid complexes at different protein:polysaccharide ratios and observed that the increase in anionic groups provided by hyaluronic acid neutralized the cationic groups of proteins leading to a negative net charge. Finally, as the NaCl concentration increased (from 0 to 100 mM), the negative charge increased, which could be due to a neutralization of the positive charge of the proteins by the chloride ions of the salt, as we explained earlier.

3.2.2. Particle size

Particle size analyses, including particle size distribution (PSD), hydrodynamic diameter (Z-average), and polydispersity index (PDI) anal-

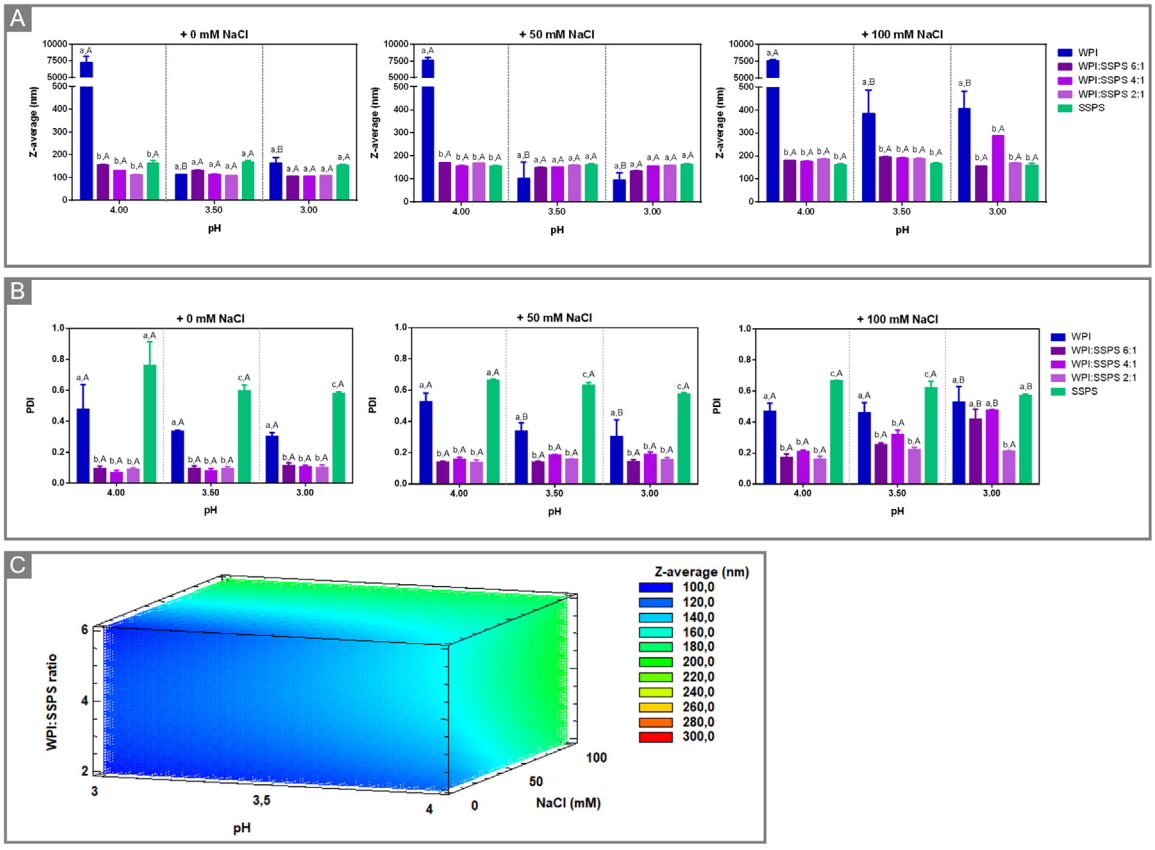

Fig. 5. (A) Z-average and (B) Polydispersity index (PDI) of WPI, SSPS, or complexes at different WPI:SSPS ratios as a function of pH and NaCl-added concentration. Different lowercase letters indicate significant differences ($p < 0.05$) between different samples at the same pH condition. Different uppercase letters indicate significant differences ($p < 0.05$) between the same sample at different pH conditions. (C) Statistical response mesh for Z-average as a function of pH, WPI:SSPS ratio, and NaCl-added concentration.

ysis, are useful tools for better understanding of biopolymers complexation and for approaching the appropriate conditions for complexation (Ghadermazi et al., 2019a). PDI is a parameter reflecting the polydispersity of the PSD of colloid suspension; generally, a PDI < 0.3 indicates a relatively homogeneously dispersed colloid suspension (Liu et al., 2020). According to Z-average and PDI measurements (Fig. 5A and B), the WPI control formed larger protein aggregates at pH 4.0 than at pH 3.5 or 3.0, which could be due to the proximity between pH and pI of proteins (Shang et al., 2021). As seen in ζ-potential measurement, WPI presented less superficial charges at pH 4.0, leading to protein aggregation into large clumps. All the WPI control samples presented PDI close to 0.5, which allows interpreting that there is high polydispersity and aggregation in these samples. This information agrees with the multimodal PSD that presented a population of small size (free protein) and other populations of larger sizes (aggregates of varied sizes). On the contrary, WPI-SSPS complexes presented nanometric sizes, independently of pH, WPI:SSPS ratio, and NaCl concentration. Similarly, Shang et al. (2021) reported the obtention of complexes between WPI and *Flammulina velutipes* polysaccharide with a lower Z-average than the respective control of WPI.

According to the statistical response mesh (Fig. 5C) and surfaces (Fig. S7), only the salt concentration significantly affected the Z-average of complexes. The Z-average increased as the NaCl concentration increased (from 0 to 100 mM). For 2:1 WPI:SSPS complexes, an analysis of the PSD shows that, regardless of the pH and NaCl concentration, the populations were monomodal and centered on the Z-average. This result suggests that the increase in the salt concentration would give rise to the swelling of these complexes instead of an aggregation process. On the same trend, the 4:1 and 6:1 WPI:SSPS complexes presented monomodal particle size distributions (PSDs) with PDI < 0.2 in absence of salt and the presence of 50 mM NaCl. However, these samples presented multimodal PSDs with PDI > 0.4 in the presence of 100 mM NaCl. These multimodal PSDs showed two populations centered around 200 nm and around 1000–1500 nm. In these cases, the increase in the salt concentration would lead to the aggregation of the complexes into larger particles and not to a swelling process. Liu et al. (2020) and Yi et al. (2021) reported an increase in the Z-average and PDI values with the increase of NaCl concentration from 0 to 200 mM for α-lactalbumin-chitosan complexes and WPI-alginate complexes, respectively. Both authors hypothesized that the reduction of electrostatic attraction between the protein and polysaccharide molecules resulted in the detachment of the polysaccharide from the complexes and the occurrence of bridging aggregation.

According to the statistical response mesh (Fig. 5C) and surfaces (Fig. S7), the pH and WPI:SSPS ratio did not significantly affect the Z-average of complexes. In the same direction, Liu et al., 2020c reported no remarkable Z-average diameter changes for α-lactalbumin and chitosan complexes in the pH range of 3.0 to 4.5. In addition, Zamani et al. (2020) described the formation of nanosized WPI-SSPS particles at pH 7.0 (non-interactive pH) and pH 3.5, and described that the Z-average remained unchanged in most of the WPI:SSPS ratios studied.

In addition to the measurements on the day of production, the Z-average was monitored during storage on days 28 and 56 post-production (Fig. S8). For the complexes, all Z-averages remained between 100 and 200 nm but, for some samples, increased significantly on days 28 and 56 compared to day 0. As the PSDs remained monomodal and centered on the Z-average, the significant increase in particle size could be due to a swelling process.

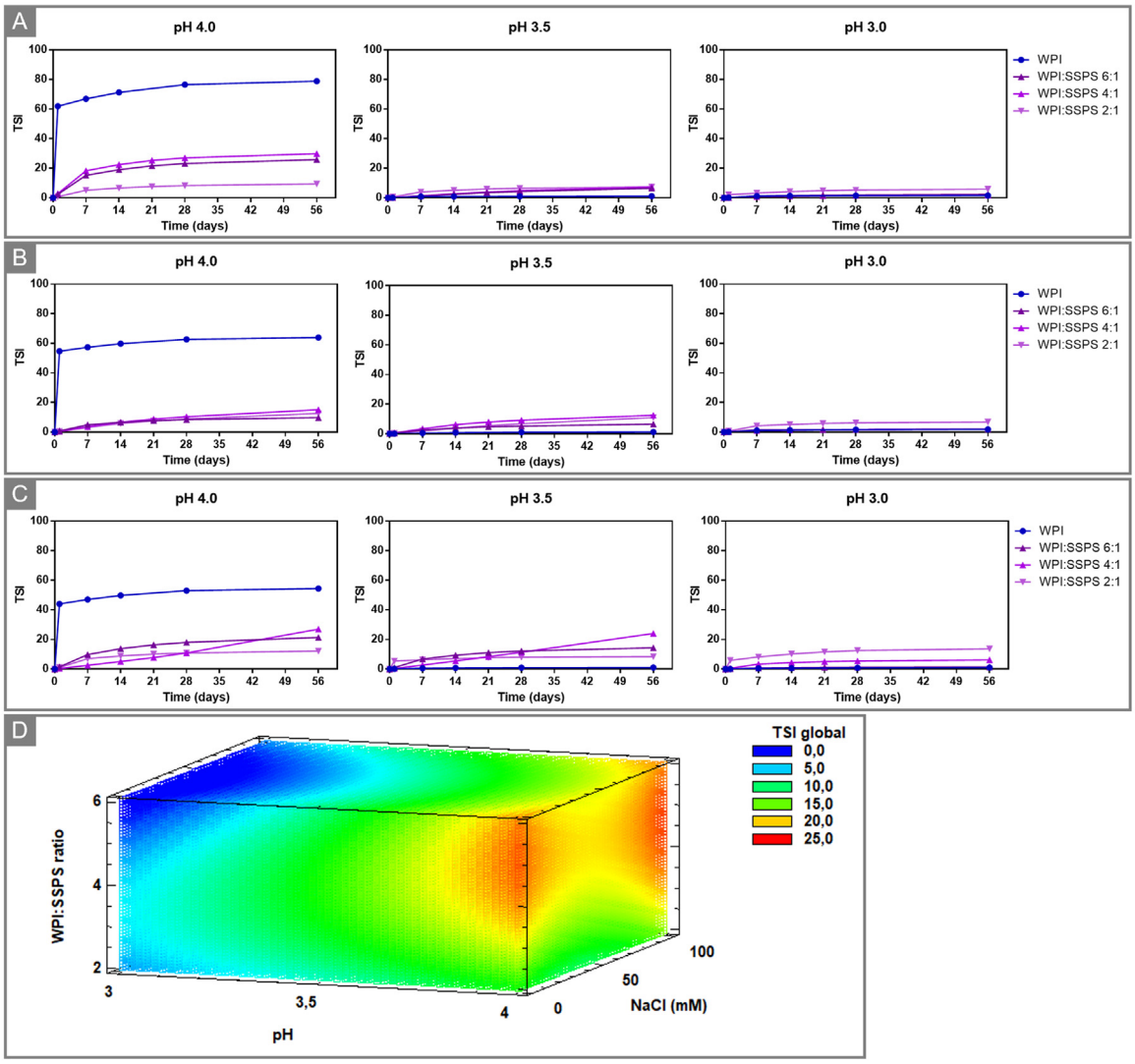

Fig. 6. Turbiscan stabilization index (TSI) of WPI, SSPS, or complexes at different WPI:SSPS ratios as function of pH and NaCl-added concentration of (A) 0 mM NaCl, (B) 50 mM NaCl, or (C) 100 mM NaCl. (D) Statistical response mesh for TSI as function of pH, WPI:SSPS ratio, and NaCl-added concentration.

3.2.3. *Physical stability*

Turbiscan technique is a helpful tool for monitoring the destabilization kinetics of a system and assessing the extent of eventual phase separation. The Turbiscan stability index (TSI) is a relative number without units that allows comparison of the relative stability of different samples based on the variations in the rate of backscattering/transmission intensity of the sample over time; the TSI is lower when the stability of the system is higher (Chevalier et al., 2019). According to TSI results (Fig. 6A–C), WPI control at pH 4.0, independently of salt concentration, presented a rapid destabilization even on the same day of preparation. In this sample, the BS increased in the bottom zone of the tube, reflecting the precipitation of the large particles. In contrast, WPI controls at pH 3.5 and pH 3.0 gave rise to translucent dispersions stable over time. Otherwise, complexes showed increased stability than the WPI control at pH 4.0 independently of pH, WPI:SSPS ratio, and salt concentration. Moreover, complexes exhibited less change in the transmission profiles and lower TSI values (smaller than 20) over space and time indicating better stability of WPI in the presence of SSPS than WPI alone. Shang et al. (2021) reported related results for WPI and *Flammulina velutipes* polysaccharide complexes that showed better Turbiscan stabilities than respective WPI controls, which are destabilized by sedimentation. In addition, Guo et al. (2019) reported TSI values for pea protein isolate significantly higher than those of pea protein isolate-propylene glycol alginate complexes.

According to the statistical mesh of response (Fig. 6D), the pH and the interaction between pH and WPI:SSPS ratio significantly affected the TSI of complexes at day 56 post-production. At pH 3.0, all samples showed a stable trend with global TSI values below 10. At pH 3.5, samples without salt addition formed stable dispersions, while samples with the addition of NaCl showed lower stability and sedimentation/clarification process. Finally, at pH 4.0, the samples with added salt presented the greatest cases of destabilization. Now, comparing the different WPI:SSPS ratios, the stability of the complexes exhibited the following increasing order: 6:1 < 4:1 < 2:1. This trend could be due to, as the concentration of SSPS increases, complexes with greater stability can be obtained since the presence of a polysaccharide interacting with the protein provided adequate electrostatic and steric repulsions due to a pectin-like structure with branches (Li et al., 2020). In the same way, Hosseini et al. (2016) informed that at higher protein:polysaccharide ratios, the β-lactoglobulin and gum acacia or carboxymethyl cellulose complexes did not exhibit any sedimentation, indicating that small stable nanocomplexes with high stability.

3.2.4. Summary of pH, WPI:SSPS ratio, and NaCl-added concentration effects

The results showed that the characteristics of the WPI-SSPS complexes can be modulated through the modification of pH, WPI:SSPS mass ratio, and salt concentration.

By lowering the pH (from 4.0 to 3.0), the ζ-potential of WPI-SSPS complexes became neutralized by the interaction of positive-charge WPI and negative-charge SSPS. Also, by lowering the pH, the WPI-SSPS complexes became stabilized, showing no sedimentation and lower TSI values.

By decreasing the WPI:SSPS ratio (from 6:1 to 2:1) i.e., by incrementing SSPS concentration, the ζ-potential of WPI-SSPS complexes became more negative because of the increment in the negative-charge SSPS available.

Finally, by increasing the NaCl concentration (from 0 to 100 mM), the ζ-potential of WPI-SSPS complexes became more negative because of the neutralization of charge groups in protein chains. In addition, by increasing the salt concentration, the Z-average of WPI-SSPS complexes was incremented through both swelling and aggregation processes.

According to the statistical optimization of responses, the complexes must be prepared under pH 3.5, 2:1 WPI:SSPS ratio, and in the absence of added salt, to present a lower Z-average and greater stability (lower TSI) with a ζ-potential close to neutrality. To further demonstrate the WPI-SSPS interaction in these optimized conditions, intrinsic protein fluorescence emission and protein surface hydrophobicity were characterized and discussed in the supplementary information (Fig. S10).

4. Conclusions

The present study demonstrates that the complex formation by electrostatic interaction between WPI and SSPS is highly dependent on the pH of the medium, the WPI:SSPS mass ratio, and the NaCl-added concentration. Moreover, the characteristics and physical stability of these WPI-SSPS complexes can be modulated by modifying the same parameters. The obtained results provide further insight into the nature of the molecular interactions in WPI-polyelectrolyte systems and allow the designing of WPI-SSPS complexes with specific characteristics of size, charge, and physical stability. Besides, since WPI-SSPS complexes presented nanometric size and high physical stability at pH 3.5 and 3.0 in low salt concentrations, WPI-SSPS complexes could be incorporated into acidic food matrices for different potential applications, such as including encapsulation of bioactive compounds, modulation of opacity in beverages, and stabilization of acid emulsions and foams. However, the novel and improved functionality of these WPI-SSPS complexes concerning WPI control must still be studied. The perspective of our group is to implement the WPI-SSPS complexes to encapsulate and stabilize curcumin in acidic beverages, studying the functionality and stability against simulated gastrointestinal digestion.

Funding

This project was supported by the National University of Quilmes (1300/19 I+D grant) and Consejo Nacional de Investigaciones Científicas y Técnicas (PIP 2021-2023, 11220200100354CO grant). The financial support is gratefully acknowledged.

Declaration of Competing Interest

The authors declare that they have no known competing financial interests or personal relationships that could have appeared to influence the work reported in this paper.

CRediT authorship contribution statement

Daniela E. Igartúa: Conceptualization, Data curation, Formal analysis, Investigation, Methodology, Writing – original draft. **Dario M. Cabezas:** Conceptualization, Funding acquisition, Methodology, Supervision, Writing – review & editing. **Gonzalo G. Palazolo:** Conceptualization, Funding acquisition, Methodology, Project administration, Supervision, Writing – review & editing.

Data Availability

Data will be made available on request.

Acknowledgments

The authors want to thank both Fuji Oil Co. Ltd (Osaka, Japan) and Arla Foods Ingredients Argentina, S.A. (Buenos Aires, Argentina) for the provision of soluble soybean polysaccharides and whey protein isolate, respectively. Gonzalo G. Palazolo, Dario M. Cabezas and Daniela E. Igartúa are members of the Scientific Research Program from the Consejo Nacional de Investigaciones Científicas y Técnicas (CONICET).

Supplementary materials

Supplementary material associated with this article can be found, in the online version, at doi:10.1016/j.focha.2022.100123.

References

Ahmad, M., Ritzoulis, C., Pan, W., & Chen, J. (2020). Chemical physics of whey protein isolate in the presence of mucin: From macromolecular interactions to functionality. *International Journal of Biological Macromolecules, 143*, 573–581. doi:10.1016/j.ijbiomac.2019.12.069.

Azarikia, F., & Abbasi, S. (2016). Mechanism of soluble complex formation of milk proteins with native gums (tragacanth and Persian gum). *Food Hydrocolloids, 59*, 35–44. doi:10.1016/j.foodhyd.2015.10.018.

Bastos, L. P. H., de Carvalho, C. W. P., & Garcia-Rojas, E. E. (2018). Formation and characterization of the complex coacervates obtained between lactoferrin and sodium alginate. *International Journal of Biological Macromolecules, 120*, 332–338. doi:10.1016/j.ijbiomac.2018.08.050.

Bédié, G. K., Turgeon, S. L., & Makhlouf, J. (2008). Formation of native whey protein isolate-low methoxyl pectin complexes as a matrix for hydro-soluble food ingredient entrapment in acidic foods. *Food Hydrocolloids, 22*(5), 836–844. doi:10.1016/j.foodhyd.2007.03.010.

Behrouzain, F., & Razavi, S. M. A. (2020). Structure-rheology relationship of basil seed gum-whey protein isolate mixture: Effect of thermal treatment and biopolymer ratio. *Food Hydrocolloids, 102*, Article 105608. doi:10.1016/j.foodhyd.2019.105608.

Behrouzain, F., Razavi, S. M. A., & Joyner, H. (2020). Mechanisms of whey protein isolate interaction with basil seed gum: Influence of pH and protein-polysaccharide ratio. *Carbohydrate Polymers, 232*, Article 115775. doi:10.1016/j.carbpol.2019.115775.

Cabezas, D. M., Pascual, G. N., Wagner, J. R., & Palazolo, G. G. (2019). Nanoparticles assembled from mixtures of whey protein isolate and soluble soybean polysaccharides. Structure, interfacial behavior and application on emulsions subjected to freeze-thawing. *Food Hydrocolloids, 95*, 445–453. doi:10.1016/j.foodhyd.2019.04.040.

Chanasattru, W., Jones, O. G., Decker, E. A., & McClements, D. J. (2009). Impact of co-solvents on formation and properties of biopolymer nanoparticles formed by heat treatment of β-lactoglobulin–Pectin complexes. *Food Hydrocolloids, 23*(8), 2450–2457. doi:10.1016/J.FOODHYD.2009.07.003.

Chen, W., Duizer, L., Corredig, M., & Goff, H. D. (2010). Addition of soluble soybean polysaccharides to dairy products as a source of dietary fiber. *Journal of Food Science, 75*(6), C478–C484. doi:10.1111/j.1750-3841.2010.01688.x.

Chevalier, L. M., Rioux, L. E., Angers, P., & Turgeon, S. L. (2019). Study of the interactions between pectin in a blueberry puree and whey proteins: Functionality and application. *Food Hydrocolloids, 87*, 61–70. doi:10.1016/J.FOODHYD.2018.07.038.

Cortés-Morales, E. A., Mendez-Montealvo, G., & Velazquez, G. (2021). Interactions of the molecular assembly of polysaccharide-protein systems as encapsulation materials. A review. *Advances in Colloid and Interface Science, 295*, Article 102398. doi:10.1016/j.cis.2021.102398.

Damodaran, S., Parkin, K. L., & Fennema, O. R. (2007). *Fennema's food chemistry*. CRC press.

Devi, N., Sarmah, M., Khatun, B., & Maji, T. K. (2017). Encapsulation of active ingredients in polysaccharide–protein complex coacervates. *Advances in Colloid and Interface Science, 239*, 136–145. doi:10.1016/j.cis.2016.05.009.

Fioramonti, S. A., Perez, A. A., Aríngoli, E. E., Rubiolo, A. C., & Santiago, L. G. (2014). Design and characterization of soluble biopolymer complexes produced by electrostatic self-assembly of a whey protein isolate andsodium alginate. *Food Hydrocolloids, 35*, 129–136. doi:10.1016/j.foodhyd.2013.05.001.

Gaber, M., Mabrouk, M. T., Freag, M. S., Khiste, S. K., Fang, J. Y., Elkhodairy, K. A., & Elzoghby, A. O. (2018). Protein-polysaccharide nanohybrids: Hybridization techniques and drug delivery applications. *European Journal of Pharmaceutics and Biopharmaceutics, 133*, 42–62. doi:10.1016/j.ejpb.2018.10.001.

Gentés, M. C., St-Gelais, D., & Turgeon, S. L. (2010). Stabilization of whey protein Isolate-pectin complexes by heat. *Journal of Agricultural and Food Chemistry, 58*(11), 7051–7058. doi:10.1021/jf100957b.

Gentile, L. (2020). Protein–polysaccharide interactions and aggregates in food formulations. *Current Opinion in Colloid and Interface Science, 48*, 18–27. doi:10.1016/j.cocis.2020.03.002.

Ghadermazi, R., Khosrowshahi Asl, A., & Tamjidi, F. (2019a). Optimization of whey protein isolate-quince seed mucilage complex coacervation. *International Journal of Biological Macromolecules, 131*, 368–377. doi:10.1016/j.ijbiomac.2019.03.026.

Ghadermazi, R., Khosrowshahi Asl, A., & Tamjidi, F. (2020b). Complexation and coacervation of whey protein isolate with quince seed mucilage. *Journal of Dispersion Science and Technology*, 1–10. doi:10.1080/01932691.2020.1822862.

Girard, M., Sanchez, C., Laneuville, S. I., Turgeon, S. L., & Gauthier, S. F. (2004). Associative phase separation of β-lactoglobulin/pectin solutions: A kinetic study by small angle static light scattering. *Colloids and Surfaces B Biointerfaces, 35*(1), 15–22. doi:10.1016/j.colsurfb.2004.02.002.

Goh, K. K. T., Teo, A., Sarkar, A., & Singh, H. (2019). Milk protein-polysaccharide interactions. In *Milk proteins: from expression to food* (pp. 499–535). Elsevier. doi:10.1016/B978-0-12-815251-5.00013-X.

Gorji, E. G., Waheed, A., Ludwig, R., Toca-Herrera, J. L., Schleining, G., & Gorji, S. G. (2018). Complex coacervation of milk proteins with sodium alginate. *Journal of Agricultural and Food Chemistry, 66*(12), 3210–3220. doi:10.1021/acs.jafc.7b03915.

Guo, Q., Su, J., Yuan, F., Mao, L., & Gao, Y. (2019). Preparation, characterization and stability of pea protein isolate and propylene glycol alginate soluble complexes. *LWT, 101*, 476–482. doi:10.1016/j.lwt.2018.11.057.

Hadian, M., Hosseini, S. M. H., Farahnaky, A., Mesbahi, G. R., Yousefi, G. H., & Saboury, A. A. (2016). Isothermal titration calorimetric and spectroscopic studies of β-lactoglobulin-water-soluble fraction of Persian gum interaction in aqueous solution. *Food Hydrocolloids, 55*, 108–118. doi:10.1016/j.foodhyd.2015.11.006.

Hosseini, S. M. H., Emam-Djomeh, Z., Negahdarifar, M., Sepeidnameh, M., Razavi, S. H., & Van der Meeren, P. (2016). Polysaccharide type and concentration affect nanocomplex formation in associative mixture with β-lactoglobulin. *International Journal of Biological Macromolecules, 93*, 724–730. doi:10.1016/j.ijbiomac.2016.09.037.

Hu, J., Zhao, T., Li, S., Wang, Z., Wen, C., Wang, H., Yu, C., & Ji, C. (2019). Stability, microstructure, and digestibility of whey protein isolate – Tremella fuciformis polysaccharide complexes. *Food Hydrocolloids, 89*, 379–385. doi:10.1016/j.foodhyd.2018.11.005.

Jia, X., Chen, M., Wan, J. B., Su, H., & He, C. (2015). Review on the extraction, characterization and application of soybean polysaccharide. *RSC Advances, 5*(90), 73525–73534. doi:10.1039/c5ra12421b.

Jones, O., Decker, E. A., & McClements, D. J. (2010). Thermal analysis of β-lactoglobulin complexes with pectins or carrageenan for production of stable biopolymer particles. *Food Hydrocolloids, 24*(2–3), 239–248. doi:10.1016/j.foodhyd.2009.10.001.

Jones, O. G., & McClements, D. J. (2011). Recent progress in biopolymer nanoparticle and microparticle formation by heat-treating electrostatic protein-polysaccharide complexes. In *Advances in colloid and interface science: 167* (pp. 49–62). Elsevier. Issues. doi:10.1016/j.cis.2010.10.006.

Klemmer, K. J., Waldner, L., Stone, A., Low, N. H., & Nickerson, M. T. (2012). Complex coacervation of pea protein isolate and alginate polysaccharides. *Food Chemistry, 130*(3), 710–715. doi:10.1016/j.foodchem.2011.07.114.

Kong, F., Kang, S., Zhang, J., Jiang, L., Liu, Y., Yang, M., Cao, X., Zheng, Y., Shao, J., & Yue, X. (2022). The non-covalent interactions between whey protein and various food functional ingredients. *Food Chemistry, 394*, Article 133455. doi:10.1016/J.FOODCHEM.2022.133455.

Lan, Y., Chen, B., & Rao, J. (2018a). Pea protein isolate–high methoxyl pectin soluble complexes for improving pea protein functionality: Effect of pH, biopolymer ratio and concentrations. *Food Hydrocolloids, 80*, 245–253. doi:10.1016/j.foodhyd.2018.02.021.

Lan, Y., Ohm, J. B., Chen, B., & Rao, J. (2020b). Phase behavior, thermodynamic and microstructure of concentrated pea protein isolate-pectin mixture: Effect of pH, biopolymer ratio and pectin charge density. *Food Hydrocolloids, 101*, Article 105556. doi:10.1016/j.foodhyd.2019.105556.

Lan, Y., Ohm, J. B., Chen, B., & Rao, J. (2020b). Phase behavior and complex coacervation of concentrated pea protein isolate-beet pectin solution. *Food Chemistry, 307*, Article 125536. doi:10.1016/j.foodchem.2019.125536.

Li, H., Wang, T., Hu, Y., Wu, J., & Van der Meeren, P. (2022). Designing delivery systems for functional ingredients by protein/polysaccharide interactions. *Trends in Food Science and Technology, 119*, 272–287. doi:10.1016/j.tifs.2021.12.007.

Li, H., Yuan, Y., Zhu, J., Wang, T., Wang, D., & Xu, Y. (2020). Zein/soluble soybean polysaccharide composite nanoparticles for encapsulation and oral delivery of lutein. *Food Hydrocolloids, 103*, Article 105715. doi:10.1016/j.foodhyd.2020.105715.

Liu, J., Shim, Y. Y., & Reaney, M. J. T. (2020). Ionic strength and hydrogen bonding effects on whey protein isolate–flaxseed gum coacervate rheology. *Food Science and Nutrition, 8*(4), 2102–2111. doi:10.1002/fsn3.1504.

Liu, K., Zha, X. Q., Shen, W. Di, Li, Q. M., Pan, L. H., & Luo, J. P (2020). The hydrogel of whey protein isolate coated by lotus root amylopectin enhance the stability and bioavailability of quercetin. *Carbohydrate Polymers, 236*, Article 116009. doi:10.1016/j.carbpol.2020.116009.

Liu, S., Low, N. H., & Nickerson, M. T. (2009). Effect of pH, salt, and biopolymer ratio on the formation of pea protein isolate gum arabic complexes. *Journal of Agricultural and Food Chemistry, 57*(4), 1521–1526. doi:10.1021/jf802643n.

Liu, Y., Gao, L., Yi, J., Fan, Y., Wu, X., & Zhang, Y. (2020). α-Lactalbumin and chitosan core-shell nanoparticles: resveratrol loading, protection, and antioxidant activity. *Food and Function, 11*(2), 1525–1536. doi:10.1039/c9fo01998g.

Madureira, A. R., Pereira, C. I., Gomes, A. M. P., Pintado, M. E., & Xavier Malcata, F. (2007). Bovine whey proteins - overview on their main biological properties. *Food Research International, 40*(10), 1197–1211. doi:10.1016/j.foodres.2007.07.005.

Maeda, H., & Nakamura, A. (2009). Soluble soybean polysaccharide. In *Handbook of hydrocolloids* (pp. 693–709). Elsevier. doi:10.1533/9781845695873.693.

Nakamura, A., Yoshida, R., Maeda, H., Furuta, H., & Corredig, M. (2004). Study of the role of the carbohydrate and protein moieties of soy soluble polysaccharides in their emulsifying properties. *Journal of Agricultural and Food Chemistry, 52*(17), 5506–5512.

Phillips, G. O., & Williams, P. A. (2011). Handbook of Food Proteins. *Handbook of food proteins*. Elsevier. doi:10.1533/9780857093639.

Rocha-Mendoza, D., Kosmerl, E., Krentz, A., Zhang, L., Badiger, S., Miyagusuku-Cruzado, G., Mayta-Apaza, A., Giusti, M., Jiménez-Flores, R., & García-Cano, I. (2021). Invited review: Acid whey trends and health benefits. *Journal of Dairy Science, 104*(2), 1262–1275. doi:10.3168/jds.2020-19038.

Rodriguez Patino, J. M., & Pilosof, A. M. R. (2011). Protein-polysaccharide interactions at fluid interfaces. *Food Hydrocolloids, 25*(8), 1925–1937. doi:10.1016/j.foodhyd.2011.02.023.

Sanchez, C., Mekhloufi, G., & Renard, D. (2006). Complex coacervation between β-lactoglobulin and acacia gum: A nucleation and growth mechanism. *Journal of Colloid and Interface Science, 299*(2), 867–873. doi:10.1016/j.jcis.2006.02.031.

Shang, J., Liao, M., Jin, R., Teng, X., Li, H., Xu, Y., Zhang, L., & Liu, N. (2021). Molecular properties of flammulina velutipes polysaccharide–whey protein isolate (Wpi) complexes via noncovalent interactions. *Foods, 10*(1). doi:10.3390/foods10010001.

Stone, A. K., & Nickerson, M. T. (2012). Formation and functionality of whey protein isolate-(kappa-, iota-, and lambda-type) carrageenan electrostatic complexes. *Food Hydrocolloids, 27*(2), 271–277. doi:10.1016/j.foodhyd.2011.08.006.

Wagoner, T. B., & Foegeding, E. A. (2017). Whey protein–pectin soluble complexes for beverage applications. *Food Hydrocolloids, 63*, 130–138. doi:10.1016/j.foodhyd.2016.08.027.

Weinbreck, F., Nieuwenhuijse, H., Robijn, G. W., & De Kruif, C. G. (2004). Complexation of whey proteins with carrageenan. *Journal of Agricultural and Food Chemistry, 52*(11), 3550–3555. doi:10.1021/jf034969t.

Weinbreck, F., Tromp, R. H., & De Kruif, C. G. (2004a). Composition and structure of whey protein/gum arabic coacervates. *Biomacromolecules, 5*(4), 1437–1445.

Weinbreck, F., Wientjes, R. H. W., Nieuwenhuijse, H., Robijn, G. W., & de Kruif, C. G. (2004b). Rheological properties of whey protein/gum arabic coacervates. *Journal of Rheology, 48*(6), 1215–1228.

Xu, Y. T., & Liu, L. L. (2016). Structural and functional properties of soy protein isolates modified by soy soluble polysaccharides. *Journal of Agricultural and Food Chemistry, 64*(38), 7275–7284. doi:10.1021/acs.jafc.6b02737.

Yi, J., Peng, G., Zheng, S., Wen, Z., Gan, C., & Fan, Y. (2021). Fabrication of whey protein isolate-sodium alginate nanocomplex for curcumin solubilization and stabilization in a model fat-free beverage. *Food Chemistry, 348*, Article 129102. doi:10.1016/j.foodchem.2021.129102.

Zamani, H., Zamani, S., Zhang, Z., & Abbaspourrad, A. (2020). Exceptional colloidal stability of acidified whey protein beverages stabilized by soybean soluble polysaccharide. *Journal of Food Science, 85*(4), 989–997. doi:10.1111/1750-3841.15041.

Zhang, Q., Jeganathan, B., Dong, H., Chen, L., & Vasanthan, T. (2021). Effect of sodium chloride on the thermodynamic, rheological, and microstructural properties of field pea protein isolate/chitosan complex coacervates. *Food Chemistry, 344*, Article 128569. doi:10.1016/J.FOODCHEM.2020.128569.

Zhao, R. X., Qi, J. R., Liu, Q. R., Zeng, W. Q., & Yang, X. Q. (2018). Fractionation and characterization of soluble soybean polysaccharide esterified of octenyl succinic anhydride and its effect as a stabilizer in acidified milk drinks. *Food Hydrocolloids, 85*, 215–221. doi:10.1016/j.foodhyd.2018.07.023.

Zhong, W., Li, C., Diao, M., Yan, M., Wang, C., & Zhang, T. (2021). Characterization of interactions between whey protein isolate and hyaluronic acid in aqueous solution: Effects of pH and mixing ratio. *Colloids and Surfaces B Biointerfaces, 203*, Article 111758. doi:10.1016/j.colsurfb.2021.111758.